Journal of Alloys and Compounds 827 (2020) 154378

Contents lists available at ScienceDirect

Journal of Alloys and Compounds

journal homepage: http://www.elsevier.com/locate/jalcom

Multilayer indium saving ITO thin films produced by sputtering method

L. Voisin [a, b], M. Ohtsuka [b], S. Petrovska [c, *], R. Sergiienko [d], T. Nakamura [b]

[a] AMTC, Advanced Mining Technology Center and DIMin, Mining Engineering Department, University of Chile, Chile
[b] Institute of Multidisciplinary Research for Advanced Materials (IMRAM), Tohoku University, Sendai, 980-8577, Japan
[c] National Academy of Science of Ukraine, Frantsevich Institute for Problems of Materials Science, 3 Krzhyzhanovsky Str., Kyiv, 03142, Ukraine
[d] National Academy of Science of Ukraine, Physico-Technological Institute of Metals and Alloys, 34/1 Vernadsky Ave., Kyiv, 03142, Ukraine

ARTICLE INFO

Article history:
Received 18 November 2019
Received in revised form
10 February 2020
Accepted 14 February 2020
Available online 15 February 2020

Keywords:
Indium tin oxide
Direct current sputtering
Electrical properties
Optical properties
Surface roughness

ABSTRACT

Deposition of multilayer indium saving indium-tin oxide (ITO) thin films was attempted to achieve both low volume resistivity and high transmittance. Double-layered structures consisting of very thin layer of conventional indium tin oxide (In_2O_3-10 mass % SnO_2) and indium saving indium-tin oxide (In_2O_3-50 mass % SnO_2) layer were grown by DC sputtering on glass substrates preheated at 523 K. It was found that this method can produce polycrystalline ITO thin films having volume resistivity as low as 281 μΩcm, mobility 28 $cm^2/V \cdot s$ and carrier concentration 5.32 10^{20} cm^{-3}. Average optical transmittances exhibited above 85% in visible range of spectrum. Arithmetical mean height (S_a) and root mean square height (S_q) of films deposited at optimum conditions were 1.09 and 1.40 nm, respectively.

1. Introduction

Indium tin oxide thin films have been extensively studied due to their applications as transparent electrodes for solar cells, panel displays and for optical solar reflectors [1–4] because of their low resistivity and high transmittance. However, one significant disadvantage of the use of ITO is its high cost. There is a clear need to find a material that is more cost effective, has better or maintains properties of conventional ITO (90 mass% In_2O_3 and 10 mass% SnO_2).

Indium-saving ITO thin films were manufactured and studied in Refs. [5–15]. Utsumi et al. [5] revealed that the optimum SnO_2 concentration for sputtering of ITO thin films is 15 wt % when depositing ITO thin films with 0–100 mass% SnO_2 by magnetron sputtering. Thirumoorthi et al. [6] have studied ITO thin films with Sn concentration 0–30 mass% and found that the best electrical parameters and high optical transmittance showed film deposited at 20 mass% Sn. Biswas et al. [7,8] have investigated ITO thin films with In:Sn atomic ratios as 90:10, 70:30, 50:50 and 30:70 and showed that the lowest resistivity together with quite high transmittance demonstrated ITO thin films 70:30. Minami et al. [9] found two peaks of carrier concentration at 5–10 atomic% of Sn and at 50 atomic% of Sn and obtained ITO thin films with 50 atomic% of Sn [9–12] that possessed both low resistivity and high transmittance. The structural, electrical and optical properties of indium saving ITO thin films with ~50 mass% of SnO_2 were also studied by Li et al. [13], O'Neil et al. [14], Voisin et al. [15]. Such films with ~50 mass% of In_2O_3 are an attractive alternative to conventional ITO (90 mass% of In_2O_3) because of their lower cost due to reduced indium content.

In order to improve optical and electrical properties of indium saving ITO thin films indium saving multilayer ITO thin films can be elaborated.

ITO multilayer (ML) thin films were deposited using different methods [16–22]. In these works multilayer thin films were obtained with high conductivity and transmittance. However, such films consisted of three layers, two of which were relatively thick layers of conventional ITO. Bilayer thin films containing conventional ITO layer were manufactured and studied in Refs. [23–27].

ITO/Ga–Al doped ZnO [23] and RF-sputtered ITO/AZO and ITO/ZnO thin films [24] exhibited resistivity 3.79 × 10^{-4}, 8.4 × 10^{-4} and 1.1 × 10^{-3} Ω cm and transmittance above 90%, of 88.3 and 87.3% in visible range, respectively. However such films also contained

* Corresponding author.
E-mail address: sw.piotrowska@gmail.com (S. Petrovska).

https://doi.org/10.1016/j.jallcom.2020.154378
0925-8388/

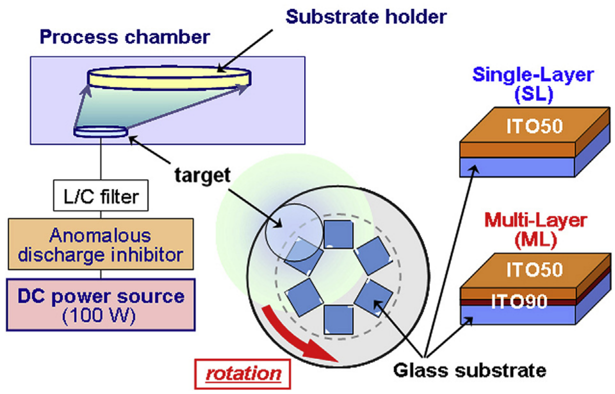

Fig. 1. Schematic diagram of the sputtering apparatus.

Table 1
Volume resistivity of ITO90 thin films deposited at optimum conditions $Q(O_2) = 0.2$ sccm on glass substrate preheated at 523 K (PHS523).

Sputtering time, min	Film thickness, nm	Volume resistivity, μΩ·cm
1.0	4.1	1014
1.5	6.2	479
2.0	8.2	425
2.5	10.3	246
3.0	12.3	217

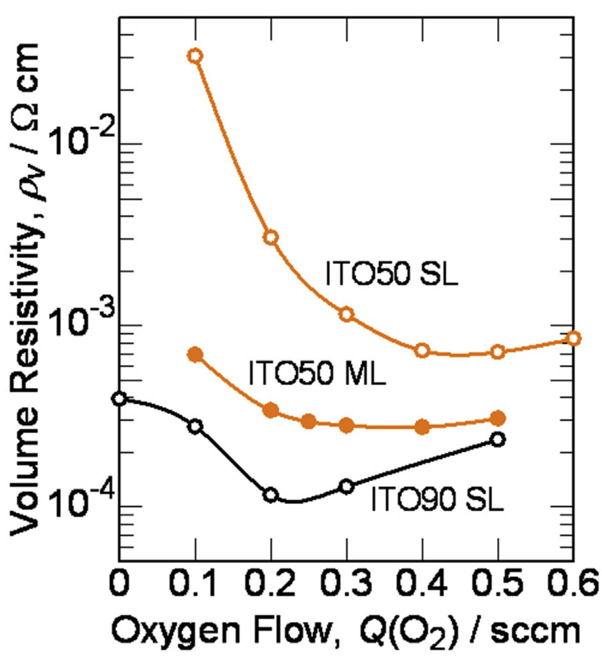

Fig. 2. Effects of oxygen flow rate on the volume resistivity of ML ITO90/ITO50 thin films, SL ITO50 thin films [15] and ITO90 thin films.

relatively thick layer (80–100 nm) of conventional ITO. ITO layer with thickness only of 20 nm was proposed to use for the fabrication of GaN-based light-emitting diodes [27]. Such 500-nm AZO/20-nm ITO bilayer films demonstrate a high transmittance above 90% in the visible region, however they have high resistivity.

In present investigation ML thin films consisting of very thin layer of conventional ITO and indium saving ITO layer were deposited onto glass substrates preheated at 523 K by DC sputtering.

Table 2
Electrical properties of as-depo. ML ITO90/ITO50 thin films in comparison with SL ITO50 thin film and ITO90 deposited at optimum conditions ($Q(O_2) = 0.2$ sccm).

Sample	Volume resistivity, ρ_V/μΩcm	Mobility, μ/ $cm^2 \cdot V^{-1} \cdot s^{-1}$	Carrier density, n/cm^{-3}
ITO90/ITO50 (ML) $Q(O_2) = 0.2/0.3$ sccm	281	28	5.32 10^{20}
ITO90/ITO50 (ML) $Q(O_2) = 0.2/0.5$ sccm	427	19.3	7.57 10^{20}
ITO50 (SL) $Q(O_2) = 0.3$ sccm	1860	12.9	2.66 10^{20}
ITO50 (SL) $Q(O_2) = 0.5$ sccm	714	40	1.57 10^{20}
ITO90 (SL) $Q(O_2) = 0.2$ sccm	110	36	1.62 10^{21}

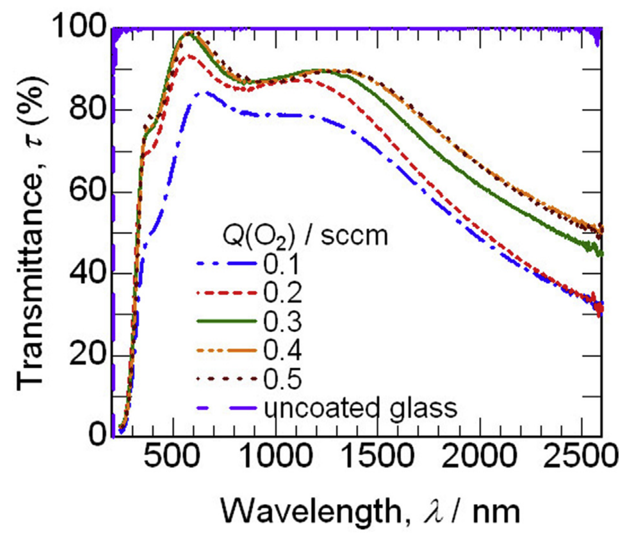

Fig. 3. Optical transmittance of as-depo. ML ITO90/ITO50 thin films deposited at $Q(O_2) = 0.2$ sccm/0.1–0.5 sccm.

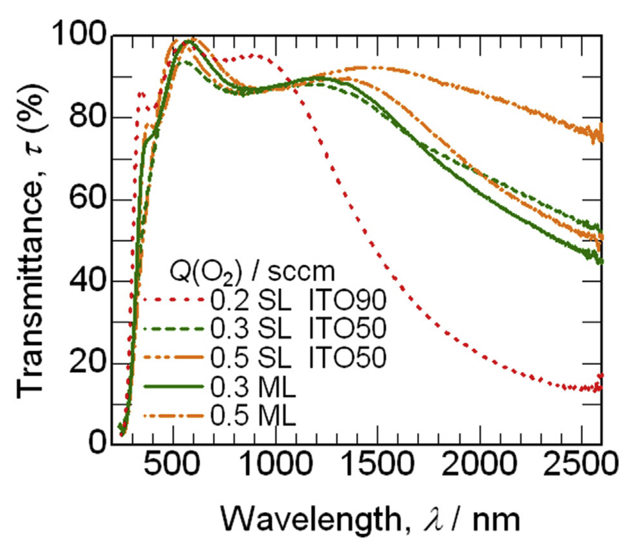

Fig. 4. Optical transmittance of as-depo. ML ITO90/ITO50 thin films deposited at $Q(O_2) = 0.2$ sccm/0.3 sccm and 0.2 sccm/0.5 sccm and SL ITO90 thin film deposited at $Q(O_2) = 0.2$ sccm and SL ITO50 thin film sputtered at $Q(O_2) = 0.3$ sccm and $Q(O_2) = 0.5$ sccm.

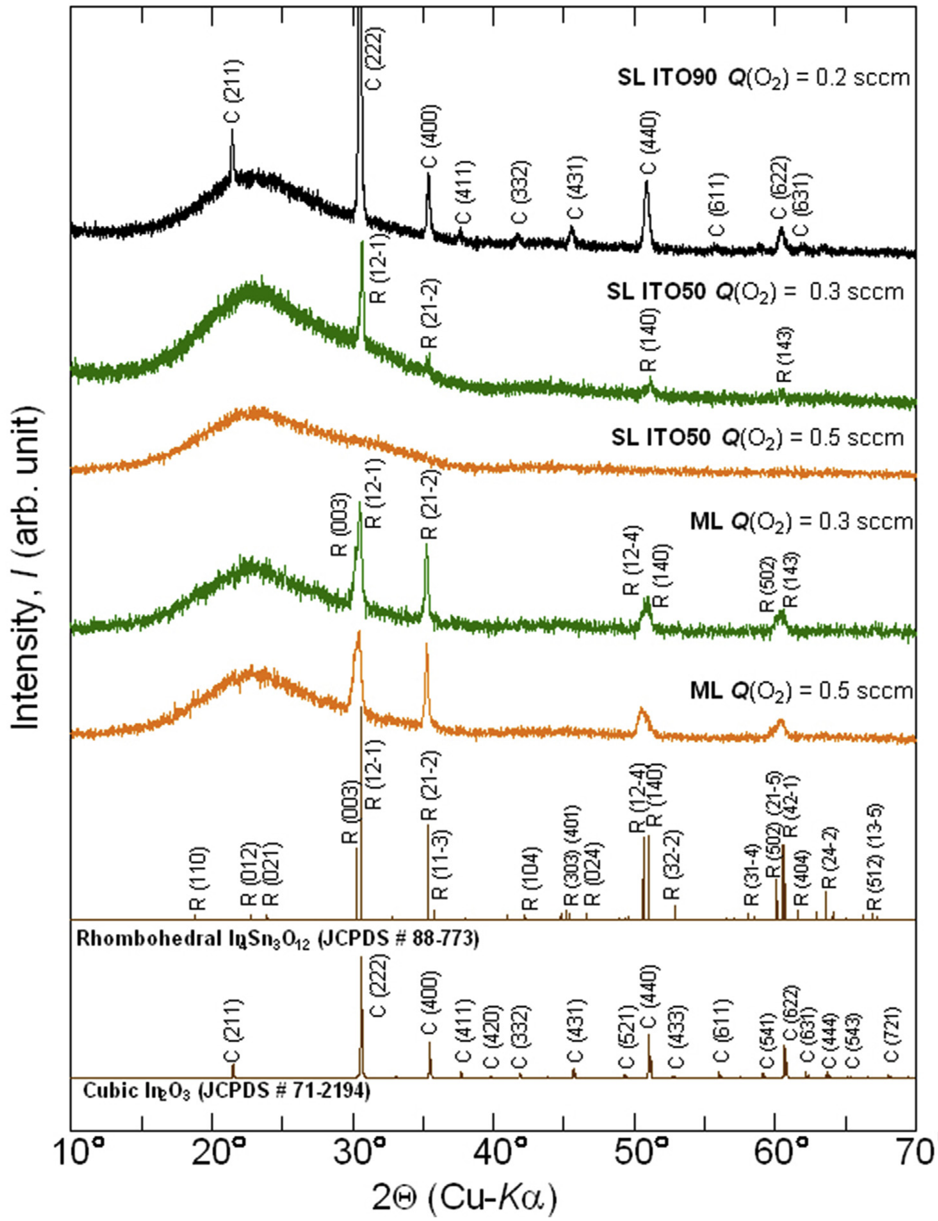

Fig. 5. X-ray diffraction (XRD) patterns of as-depo. SL and ML thin films sputtered at $Q(O_2) = 0.3$ and 0.5 sccm compared to ITO90 film with rhombohedral $In_4Sn_3O_{12}$ and cubic In_2O_3 reference data.

2. Experiment

ITO films were deposited by a commercial sputtering system ULVAC, CS-200 (Fig. 1).

The indium-tin targets containing In_2O_3 and SnO_2 in a proportion of 90:10 mass % (ITO90) and 50:50 mass % (ITO50) were used for deposition of the first and second layers, respectively. Before sputtering, the target was pre-sputtered for about 30 s with a shutter covering the target in order to remove any contaminant on the surface of the target. The DC power during the deposition was fixed at 100 W (1.23 W/cm^2). The sputtering targets dimensions were 101.6 mm (81.07 cm^2) in diameter and 5 mm in thickness.

The substrates used were the Corning EAGLE 2000 glasses (surface: 50 mm×50 mm, thickness: 0.7 mm). The process chamber was evacuated down to a pressure of 10^{-5} Pa. Total experimental pressures were resulted to be between 0.67 and 0.69 Pa. The argon gas flow introduced into the chamber was fixed at 50 sccm. The flow rate of oxygen reactive gas was set at 0.2 and 0.1–0.6 sccm for sputtering of the ITO90 and the ITO50 layer, respectively.

It is well known that ITO films deposited at a high substrate temperature show improved electrical and optical properties [28,29]. The substrate temperature was set at 523 K. The substrate holder rotated with 40 rpm in order to achieve the homogeneous deposition. Sputtering time was calculated using data for deposition rate of ITO90 and ITO50 thin films. Sputtering time for thin films was set 3 min for ITO90 as the first layer in order to obtain thickness of 12 nm and 30 min for ITO50 to get the second layer with thickness 138 nm. Thus total thickness of films was 150 nm. ITO50(0.5) ($Q(Ar)/Q(O_2) = 50$ sccm/0.5 sccm), and ITO90(0.2) ($Q(Ar)/Q(O_2) = 50$ sccm/0.2 sccm) thin films were sputtered during 32 and 37 min respectively to get thickness of 150 nm to make it possible to compare optical transmittance (τ) of SL and ML thin

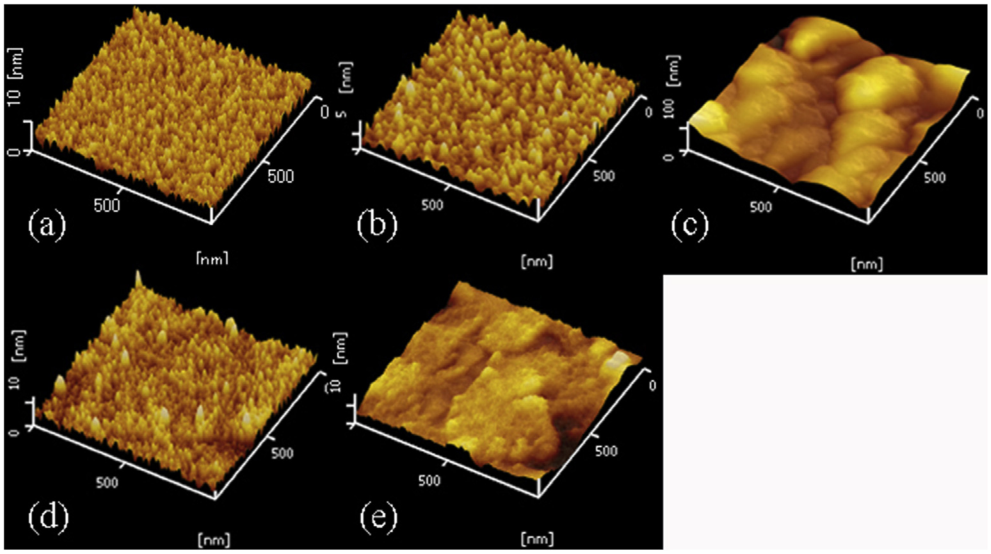

Fig. 6. Surface morphology of (a) SL ITO50 thin film deposited at $Q(O_2) = 0.3$ sccm, (b) SL ITO50 thin film deposited at $Q(O_2) = 0.5$ sccm, (c) SL ITO90 thin film deposited at $Q(O_2) = 0.2$ sccm [15], (d) ML thin films deposited at $Q(O_2) = 0.3$ and (e) ML thin films deposited at $Q(O_2) = 0.5$ sccm.

films since τ depends on films thickness [30].

The volume resistivity of ITO films was measured by a four-point probe with a resistivity meter (Mitsubishi chemical analytech, Loresta GP Model MCP-T610). Optical ttransmittance was measured in the spectral range from 200 to 2500 nm with a Hitachi High-Tech, U-4100 spectrophotometer.

The crystallinities of the ITO films were obtained from XRD measurements using Rigaku Rint-2000 difractometer with Cu$K\alpha$ (1.5418 Å) radiation.

Surface properties were investigated by a scanning probe microscope (SPM, SII L-trace II) under the DFM.

The transmission electron microscopy TEM characterization of ML ITO90/ITO50 thin films was carried out using a transmission electron microscope (Hitachi High Technology, H-9000NAR) operated at 300 kV.

It is well known that substrate plays important role in film growth and is one of the factors determined the thin film properties. To improve thin film properties it is important to choose the first layer material with high transmittance and conductivity. Such material is conventional ITO (In_2O_3 -10 mass % SnO_2). At the optimum conditions $Q(Ar)/Q(O_2) = 50/0.2$ sccm ITO90 deposited onto preheated at 523 K glass substrate showed $\rho_v = 116$ μΩcm and transmittance higher than 85%. In order to decrease usage of expensive ITO90 it was necessary to decrease the first layer thickness. To choose the optimum thickness for this layer ITO90 was sputtered during 1–3 min in order to obtain very thin films with high transmittance (of about 92%) and low resistivity (Table 1).

As can be seen from Table 1, volume resistivity decreases with increasing film thickness. As a result highly transparent and conductive layers were obtained with 12 nm thickness deposited 3 min.

3. Results and discussion

3.1. Optical and electrical properties

Fig. 2 shows volume resistivity of ML ITO90/ITO50 thin films sputtered under different flow rates. Volume resistivity of ML ITO90/ITO50 thin films decreased with increasing oxygen flow rate to 0.3 sccm and then increased. It is well known that free electrons in ITO films arise from oxygen vacancies or tin ions on substitutional sites of indium ions [31]. Therefore, resistivity has to increase by filling of oxygen vacancies through penetration of oxygen in the ITO films [32] at oxygen flow rate higher than optimum. Actually resistivity of multilayer ITO90/ITO50 thin films increased with increasing oxygen flow rate from 0.3 sccm to 0.5 sccm. However, even multilayer thin films with ITO50 layer deposited at $Q(O_2) = 0.5$ sccm showed lower volume resistivity in comparison to that of single layer ITO50.

Table 3
Root mean square height (S_q) and arithmetical mean height (S_a) of ML ITO90/ITO50, SL ITO90 and SL ITO50 thin films.

Sample	Oxygen flow $Q(O_2)$/sccm	Root mean square height, S_q/nm	Arithmetical mean height, S_a/nm
ITO90/ITO50	0.2/0.3	1.09	1.40
(ML)	0.2/0.5	1.16	1.59
ITO50 (SL)	0.3	0.86	1.09
ITO50 (SL)	0.5	0.88	1.12
ITO90 (SL)	0.2	12.8	15.7

Lower resistivity of ML ITO90/ITO50(0.3) thin films than that of SL ITO50(0.5) thin film is connected with higher carrier density of the multilayer films (Table 2) which result from the film crystallization [33].

Resistivity of ML ITO90/ITO50 thin film is somewhat higher than that of SL ITO90 thin film due to lower carrier density of the multilayer film.

Transmittance spectral measurements for ML ITO90/ITO50 thin films sputtered at different oxygen flow rates are shown in Fig. 3.

Fig. 3 shows that the transmittance in both visible and IR range noticeably increases with increasing oxygen flow rate up to 0.3 sccm. At $Q(O_2) = 0.2$ sccm/0.4 sccm τ increased noticeably only at $\lambda > 1300$ nm and keeps almost the same value under $Q(O_2) = 0.2$ sccm/0.5 sccm.

Optical transmittance τ was measured for the as-depo. SL ITO90(0.2), SL ITO50 and ML ITO90/ITO50 thin films sputtered at $Q(O_2) = 0.3$ sccm and $Q(O_2) = 0.5$ sccm (Fig. 4).

Transmittance of ML ITO90/ITO50 thin films deposited at $Q(O_2) = 0.2$ sccm/0.3 sccm and 0.2 sccm/0.5 sccm reaches 98.3 and 97.1% at $\lambda = 550$ nm, respectively. τ of ML ITO90/ITO50 thin films

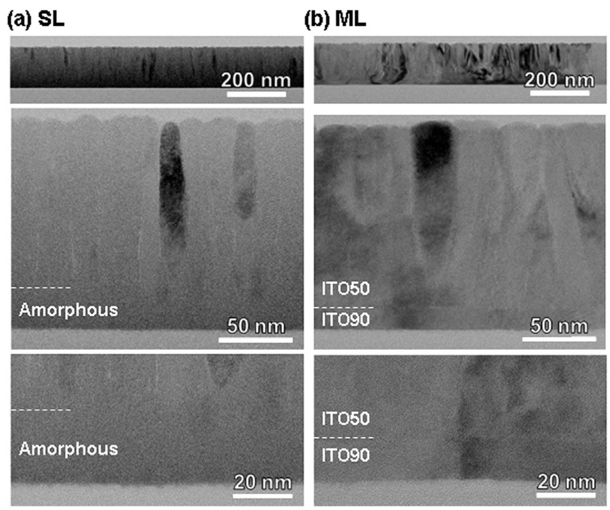

Fig. 7. Cross-sectional TEM images of (a) SL ITO50 thin film deposited at $Q(O_2) = 0.3$ sccm and (b) ML ITO90/ITO50 thin film deposited at $Q(O_2) = 0.3$ sccm. The dashed straight lines show approximate boundary between different regions.

deposited at $Q(O_2) = 0.2$ sccm/0.3 sccm is higher than that of SL ITO50 sputtered at $Q(O_2) = 0.3$ sccm at $\lambda < 1700$ nm, whereas transmittance of ML ITO90/ITO50 thin films sputtered at $Q(O_2) = 0.2$ sccm/0.5 sccm is higher than that of SL ITO50 thin film at $600<\lambda < 1000$ nm. Transmittance of ITO90 is much lower than that of ML ITO90/ITO50 thin films at $\lambda > 1100$ nm so ITO90 thin films are opaque in this wavelength range. High transmittance in the infrared range is optional for example in new transparent electrodes for QD-LED.

3.2. Structural properties

X-Ray 2θ scans were carried out from 10 to 70° (Fig. 5) and the results of those scans reveal that both as-depo. ML ITO90/ITO50 thin films and SL ITO50 thin film sputtered at $Q(Ar)/Q(O_2) = 50/0.3$ sccm show polycrystalline structure, whereas SL ITO50 thin film deposited at $Q(Ar)/Q(O_2) = 50/0.5$ sccm was amorphous. Thus ITO90 layer promoted hetero-epitaxial growth of ITO50.

As shown in Fig. 5 the results indicate that the ML ($Q(O_2) = 0.3$ and 0.5 sccm) and SL ($Q(O_2) = 0.3$ sccm) films have peaks at 30.2°, 30.5°, 35.3°, 50.7°, 51°, 60.1°, 60.4° corresponding to rhombohedral phase $In_4Sn_3O_{12}$ (JCPDS # 88−773, referred as R(hkl)) at orientation planes (003), (12-1), (21-2), (12-4), (140), (502) and (143), respectively. The peaks corresponding to reflections from atomic planes (003) and (12-1), (12-4) and (140), (502) and (143) overlap because locate very close to each other and therefore merge into three wide peaks. The presence of the rhombohedral phase $In_4Sn_3O_{12}$ phase has been confirmed in our previous articles [15,34]. The comparative ITO90 film has main peaks at 21.4°, 30.5°, 35.4°, 45.6°, 50.9° and 60.5° corresponding to cubic In_2O_3 (JCPDS # 71−2194, referred as C (hkl)) at orientation planes (211), (222), (400), (431), (440), (622), respectively. We didn't observe the rhombohedral phase In_2O_3 (JCPDS # 22−0336) which has previously been observed in thin films deposited on flexible polymer substrates in the work of Jeong et al. [35], who used an electron beam evaporator; and in transparent rhombic/cubic ITO nanocomposite thin films [36] which were deposited on glass using pulsed nebulization CVD. It can be explained by different methods and special conditions for the preparation of films. Usually the cubic In_2O_3 phase occurs more often unlike more conductive rhombohedral phase In_2O_3 in ITO films with tin compositions less than 10 mass %. Moreover the rhombohedral phase is rarely observed without applying high pressure [36].

Fig. 6 shows surface analyses taken for the as-depo. ML ITO90/ITO50(0.3, 0.5) thin films in comparison with SL ITO90(0.2) and SL ITO50(0.5) [15] by using SPM under the DFM.

Both root mean square height (S_q) and arithmetical mean height (S_a) slightly increased with increasing $Q(O_2)$ during sputtering of SL ITO50 and the second ITO50 layer of ML ITO90/ITO50 thin films (Table 3). S_a and S_q of ML ITO90/ITO50 thin films are larger than those of SL ITO50 thin films due to crystallization of multilayer films in contrast to single layer amorphous films since as it was stated above inserting an ultrathin ITO90 layer promoted crystallization of ITO50 layer.

However root mean square height (S_q) and arithmetical mean height (S_a) of ML ITO90/ITO50 are much lower than that of SL ITO90 thin film with the same thickness.

Fig. 7 shows cross-sectional TEM images of the ML ITO90/

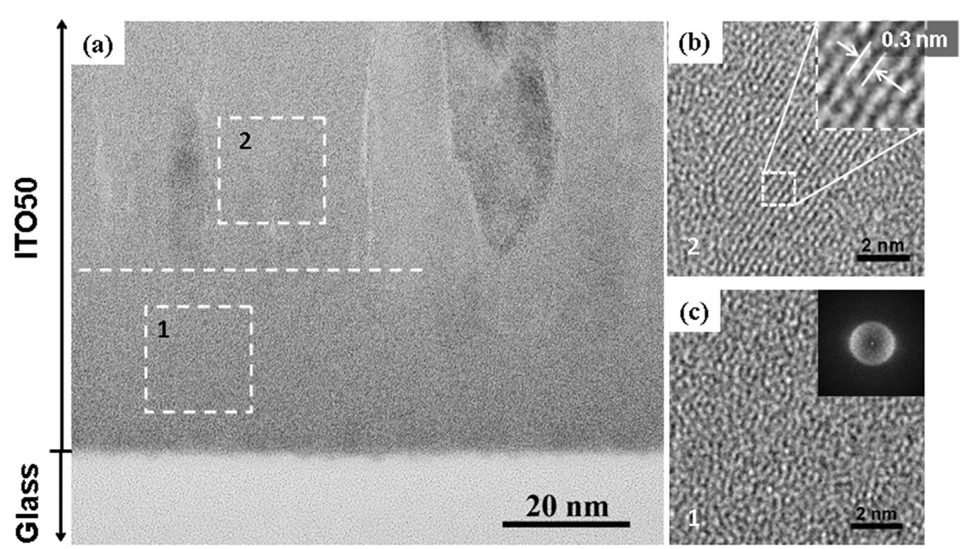

Fig. 8. (a) Cross-sectional HRTEM image of SL ITO50 thin film deposited at $Q(O_2) = 0.3$ sccm. (b) and (c) The enlarged high resolution images of the crystalline (b) and amorphous (c) regions surrounded by the dashed rectangles 1 and 2 in Fig. 8(a), respectively.

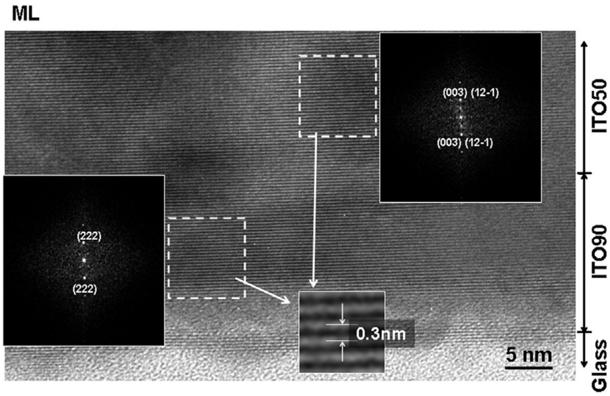

Fig. 9. Cross-sectional HRTEM image and FTT patterns of ML ITO90/ITO50 thin film deposited at Q(O_2) = 0.3 sccm. The digital diffractograms computed by Fast Fourier Transformation of the areas surrounded by dashed rectangles and the enlarged high resolution image of crystal lattice.

ITO50(0.3) thin film with 150 nm thickness compared to SL ITO50(0.3) thin film. From these results it is clear that single layer ITO50(0.3) thin film consists of two regions (Figs. 7a and 8a). The first one near glass substrate possesses most likely to be amorphous structure (Fig. 8c) with thickness is about 30 nm, which can be explained by addition stress of the first atomic layers of the deposited film. The second region consists of the individual crystalline columns (Fig. 8b).

Two layers in the multilayer film are clearly seen in Fig. 7b: the first layer is about 14 nm thick, while the second layer shows the columnar vertical growth and thickness is about 136 nm. Fig. 9 shows HRTEM image of ML ITO90/ITO50(0.3) thin film deposited onto preheated at 523 K substrate. It was performed the detailed investigation of the film in two regions – near the glass substrate and region of individual columns using Fast Fourier Transformation (FFT). The FFT analysis of high resolution image from the crystalline layers of films in Figs. 5b and 6 showed the sequence of diffraction spots from crystal planes with the lattice d-spacings of about 0.3 nm. This interlayer distance can corresponds to the standard value of 0.29205 nm (222) for the bcc lattice of indium oxide In_2O_3 (JCPDS card # 71–2194) [37] of the first ITO90(0.2) layer and the standard values of 0.2923 nm (12-1), 0.29528 nm (003) for the rhombohedral lattice of indium-tin oxide $In_4Sn_3O_{12}$ (JCPDS card # 88–773) of the second ITO50(0.3) layer [38]. Thereby high-resolution TEM investigations confirmed the XRD analysis results and both methods showed a high crystallinity of as-deposited ML ITO90/ITO50 films.

4. Conclusions

In summary, we have reported a simple technique for preparing multilayer ITO90/ITO50 thin films. In order to reduce indium usage in ITO films, an amount of indium oxide in the target was decreased from 90 to 50 mass%. DC sputtering onto preheated at 523 K glass substrates at different oxygen flow rates was used with the absence of any post-deposition heat treatment.

The optimum oxygen flow rate was found to be 0.2 sccm and 0.3 sccm for deposition of ITO90 and ITO50 layers, respectively. At the optimum oxygen flow rate as-deposited ML ITO90/ITO50 films exhibit decrease of the volume resistivity (281 μΩcm) in comparison with that of SL ITO50 films (714 μΩcm). This effect can be associated with good crystallinity of the as-deposited ML ITO90/ITO50 thin films and therefore more than threefold increase of carrier density in comparison with the as-deposited SL ITO50 thin films. Transmittance at λ = 550 nm of ML ITO90/ITO50 thin film sputtered at optimum oxygen flow rate is 98.3%. ML ITO90/ITO50 thin films show polycrystalline structure. Roughness of ML ITO90/ITO50 thin films increased with increasing Q(O_2) during sputtering of the second ITO50 layer. Arithmetical mean height (S_a) and root mean square height (S_q) of ML ITO90/ITO50 films deposited at optimum conditions were 1.09 and 1.40 nm, respectively that is significantly lower than roughness of SL ITO90 thin film with the same thickness.

The material costs for multilayer ITO90/ITO50 films offer an economical advantage over the use of conventional ITO.

Declaration of competing interest

The authors declare that they have no known competing financial interests or personal relationships that could have appeared to influence the work reported in this paper.

CRediT authorship contribution statement

L. Voisin: Conceptualization, Methodology, Investigation. **M. Ohtsuka:** Conceptualization, Methodology, Writing - review & editing, Supervision. **S. Petrovska:** Investigation, Writing - original draft. **R. Sergiienko:** Investigation, Writing - original draft. **T. Nakamura:** Supervision.

Acknowledgments

The present research was supported by New Energy and Industrial Technology Development Organization (NEDO), Japan.

References

[1] S.-Y. Lien, Characterization and optimization of ITO thin films for application in heterojunction silicon solar cells, Thin Solid Films 518 (2010) S10–S13, https://doi.org/10.1016/j.tsf.2010.03.023.
[2] U. Betz, M. Kharrazi Olsson, J. Marthy, M.F. Escolá, F. Atamny, Thin films engineering of indium tin oxide: large area flat panel displays application, Surf. Coating. Technol. 200 (2006) 5751–5759, https://doi.org/10.1016/j.surfcoat.2005.08.144.
[3] K.P. Sibin, N. Swain, P. Chowdhury, A. Dey, N. Sridhara, H.D. Shashikala, A.K. Sharma, H.C. Barshilia, Optical and electrical properties of ITO thin films sputtered on flexible FEP substrate as passive thermal control system for space applications, Sol. Energy Mater. Sol. Cells 145 (2016) 314–322, https://doi.org/10.1016/j.solmat.2015.10.035.
[4] P. Dai, J. Lu, M. Tan, Q. Wang, Y. Wu, L. Ji, L. Bian, S. Lu, H. Yang, Transparent conducting indium-tin-oxide (ITO) film as full front electrode in III–V compound solar cell, Chin. Phys. B 26 (2017), https://doi.org/10.1088/1674-1056/26/3/037305, 037305-1-037305-5.
[5] K. Utsumi, H. Iigusa, R. Tokumaru, P.K. Song, Y. Shigesato, Study on In2O3–SnO2transparent and conductive films prepared by d.c. sputtering usinghigh density ceramic targets, Thin Solid Films 445 (2003) 229–234, https://doi.org/10.1016/S0040-6090(03)01167-2.
[6] M. Thirumoorthi, J. Thomas Joseph Prakash, Structure, optical and electrical properties of indium tin oxide ultrathin films prepared by jet nebulizerspray pyrolysis technique, J. Asian Ceram. Soc. 4 (2016) 124–132, https://doi.org/10.1016/j.jascer.2016.01.001.
[7] P.K. Biswas, A. De, K. Ortner, S. Korder, Study of sol–gel-derived high tin content indium tin oxide (ITO) films on silica-coated soda lime silica glass, Mater. Lett. 58 (2004) 1540–1545, https://doi.org/10.1016/j.matlet.2003.10.023.
[8] P.K. Biswas, A. De, N.C. Pramanika, P.K. Chakraborty, K. Ortner, V. Hock, S. Korder, Effects of tin on IR reflectivity, thermal emissivity, hall mobility andplasma wavelength of sol–gel indium tin oxide films on glass, Mater. Lett. 57 (2003) 2326–2332, https://doi.org/10.1016/S0167-577X(02)01220-X.
[9] T. Minami, Y. Takeda, S. Takata, T. Kakumu, Preparation of transparent conducting In4Sn3O12thin films by DC magnetron sputtering, Thin Solid Films 309 (1997) 13–18, https://doi.org/10.1016/S0040-6090(97)00530-0.
[10] T. Minami, Transparent and conductive multicomponent oxide films prepared by magnetron sputtering, J. Vac. Sci. Technol., A 17 (1999) 1765–1772, https://doi.org/10.1116/1.581888.
[11] T. Minami, T. Kakumu, K. Shimokawa, S. Takata, New transparent conducting ZnO–In O –SnO thin films prepared by magnetron sputtering, Thin Solid Films 317 (1998) 318–321, https://doi.org/10.1016/S0040-6090(97)00547-6.
[12] T. Minami, T. Miyata, T. Yamamoto, Work function of transparent conducting

multicomponent oxide thin films prepared by magnetron sputtering, Surf. Coating. Technol. 108–109 (1998) 583–587, https://doi.org/10.1016/S0257-8972(98)00592-1.
[13] S. Li, X. Qiao, J. Chen, Effects of oxygen flow on the properties of indium tin oxide films, Mater. Chem. Phys. 98 (2006) 144–147, https://doi.org/10.1016/j.matchemphys.2005.09.012.
[14] D.H. O'Neil, V.L. Kuznetsov, R.M.J. Jacobs, M.O. Jones, P.P. Edwards, Structural, optical and electrical properties of $In_4Sn_3O_{12}$ films prepared by pulsed laser deposition, Mater. Chem. Phys. 123 (2010) 152–159, https://doi.org/10.1016/j.matchemphys.2010.03.075.
[15] L. Voisin, M. Ohtsuka, S. Petrovska, R. Sergiienko, T. Nakamura, Structural, optical and electrical properties of DC sputtered indium saving indium-tin oxide (ITO) thin films, Optik 156 (2018) 728–737, https://doi.org/10.1016/j.ijleo.2017.12.021.
[16] K.H. Choi, J.Y. Kim, Y.S. Lee, H.J. Kim, ITO/Ag/ITO multilayer films for the application of a very low resistance transparent electrode, Thin Solid Films 341 (1999) 152–155, https://doi.org/10.1016/S0040-6090(98)01556-9.
[17] Y.S. Kim, J.H. Park, D.H. Choi, H.S. Jang, J.H. Lee, H.J. Park, J.I. Choi, D.H. Ju, J.Y. Lee, D. Kim, ITO/Au/ITO multilayer thin films for transparent conducting electrode applications, Appl. Surf. Sci. 254 (2007) 1524–1527, https://doi.org/10.1016/j.apsusc.2007.07.080.
[18] M. Bender, W. Seelig, C. Daube, H. Frankenberger, B. Ocker, J. Stollenwerk, Dependence of film composition and thicknesses on optical and electrical properties of ITO–metal–ITO multilayers, Thin Solid Films 326 (1998) 67–71, https://doi.org/10.1016/S0040-6090(98)00520-3.
[19] C. Guille, J. Herrero, ITO/metal/ITO multilayer structures based on Ag and Cu metal films for high-performance transparent electrodes, Sol. Energy Mater. Sol. Cells 92 (2008) 938–941, https://doi.org/10.1016/j.solmat.2008.02.038.
[20] J.H. Park, J.H. Chae, D. Kim, Influence of nickel thickness on the properties of ITO/Ni/ITO thin films, J. Alloys Compd. 478 (2009) 330–333, https://doi.org/10.1016/j.jallcom.2008.11.065.
[21] M. Chakaroun, B. Lucas, B. Ratier, M. Aldissi, ITO/Au/ITO multilayer electrodes for CuPc/C60 solar cells, Energy Procedia 31 (2012) 102–109, https://doi.org/10.1016/j.egypro.2012.11.171.
[22] O.I. Davydova, A.V. Agafonov, Growth of optically active multilayer metal oxide films on a plastic substrate, Inorg. Mater. 52 (2016) 962–967, https://doi.org/10.1134/S002016851609003X.
[23] Y.S. Jung, H.W. Choi, K.H. Kim, Properties of ITO/Ga-Al doped ZnO bilayer thin film for saving ITO material, Mol. Cryst. Liq. Cryst. 602 (2014) 17–25, https://doi.org/10.1080/15421406.2014.944363.
[24] M.N. Rezaie, N. Manavizadeh, E. Mohammadi N. Abadi, E. Nadimi, F.A. Boroumand, Comparison study of transparent RF-sputtered ITO/AZO and ITO/ZnO bilayers for near UV-OLED applications, Appl. Surf. Sci. 392 (2017) 549–556, https://doi.org/10.1016/j.apsusc.2016.09.080.
[25] Y. Cong, D. Han, J. Dong, S. Zhang, X. Zhang, Y. Wang, Fully transparent high performance thin film transistors with bilayer ITO/Al-Sn-Zn-O channel structures fabricated on glass substrate, Sci. Rep. 7 (2017) 1497, https://doi.org/10.1038/s41598-017-01691-7.
[26] C. Wang, Y. Mao, X. Zeng, Properties of ITO–AZO bilayer thin films prepared by magnetron sputtering for applications in thin-film silicon solar cells, Appl. Phys. A 110 (2013) 41–45, https://doi.org/10.1007/s00339-012-7431-3.
[27] D. Chen, J. Lu, R. Lu, L. Chen, Z. Ye, High-Performance GaN-based LEDs with AZO/ITO thin films as transparent contact layers, IEEE Trans. Electron. Dev. 64 (2017) 2549–2555, https://doi.org/10.1109/TED.2017.2693499.
[28] L. Bo, C. Shuying, Properties of indium tin oxide films deposited by RF magnetron sputtering at various substrate temperatures, Micro & Nano Lett. 7 (2012) 835–837, https://doi.org/10.1049/mnl.2012.0454.
[29] X. Juan, Y.Y. Jie, W. Fang, Z. Kailiang, Influence of substrate temperature on properties of indium tin oxide thin films prepared by DC magnetron sputtering, ECS Trans 44 (2012) 1311–1316, https://doi.org/10.1149/1.3694465.
[30] K.J. Kumar, N.R.C. Raju, A. Subrahmanyam, Thickness dependent physical and photocatalytic properties of ITO thin films prepared by reactive DC magnetron sputtering, Appl. Surf. Sci. 257 (2011) 3075–3080, https://doi.org/10.1016/j.apsusc.2010.10.119.
[31] G. Frank, H. Kostlin, Electrical properties and defect model of tin-doped indium oxide layers, Appl. Phys. Solid Surface. 27 (1982) 197–206, https://doi.org/10.1007/BF00619080.
[32] S. Takayama, T. Sugawara, A. Tanaka, T. Himuro, Indium tin oxide films with low resistivity and low internal stress, J. Vac. Sci. Technol., A 21 (4) (2003) 1351–1354, https://doi.org/10.1116/1.1563623.
[33] M.T. Bhatti, A.M. Rana, A.F. Khan, Characterization of rf-sputtered indium tin oxide thin films, Mater. Chem. Phys. 84 (2004) 126–130, https://doi.org/10.1016/j.matchemphys.2003.11.022.
[34] M. Ohtsuka, R. Sergiienko, S. Petrovska, B. Ilkiv, T. Nakamura, Iron-doped indium saving indium-tin oxide (ITO) thin films sputtered on preheated substrates, Optik 179 (2019) 19–28, https://doi.org/10.1016/j.ijleo.2018.10.130.
[35] W.-L. Jeong, J.-H. Min, H.-M. Kwak, Y.-J. Jeon, et al., A highly conductive and flexible metal mesh/ultrathin ITO hybrid transparent electrode fabricated using low-temperature crystallization, J. Alloys Compd. 794 (2019) 114–119, https://doi.org/10.1016/j.jallcom.2019.04.249.
[36] L.A. Dunlop, A. Kursumovic, J.L. MacManus-Driscoll, Highly conducting, transparent rhombic/cubic indium tin oxide nanocomposite thin films, Cryst. Growth Des. 10 (2010) 1730–1735, https://doi.org/10.1021/cg901384d.
[37] M. Marezio, Refinement of the crystal structure of In_2O_3 at two wavelengths, Acta Crystallogr. 20 (1966) 723–728, https://doi.org/10.1107/S0365110X66001749.
[38] N. Nadaud, M. Nanot, J. Jove, T. Roisnel, A structural study of tin-doped indium oxide (ITO) ceramics using119Sn Mössbauer spectroscopy and neutron diffraction, Key Eng. Mater. 132 (1997) 1373–1376, https://doi.org/10.4028/www.scientific.net/KEM.132-136.1373.